J|A|C|S ARTICLES

Published on Web 12/02/2009

Highly Birefringent Cyanoaurate Coordination Polymers: The Effect of Polarizable C−X Bonds (X = Cl, Br)

Michael J. Katz and Daniel B. Leznoff*

Department of Chemistry, Simon Fraser University, 8888 University Drive, Burnaby, BC, Canada V5A 1S6

Received September 4, 2009; E-mail: dleznoff@sfu.ca

Abstract: Four new coordination polymers, Mn(Clterpy)$[Au(CN)_2]_2$ (Clterpy = 4′-chloro-2,2′;6′,2″-terpyridine), Mn(Brterpy)$[Au(CN)_2]_2$ (Brterpy = 4′-bromo-2,2′;6′,2″-terpyridine), Pb(Clterpy)$[Au(CN)_2]_2$, and Pb(Brterpy)-$(\mu-OH_2)_{0.5}[Au(CN)_2]_2$ were synthesized and structurally characterized, and their birefringence values were measured. The supramolecular structures of the two Mn(II) polymers are the same: they form one-dimensional (1D) chains of Mn(Xterpy)$[Au(CN)_2]_2$ units (X = Cl, Br), each having one bridging and one terminal $Au(CN)_2^-$. The Pb(II) analogues form 1D polymers containing chains of Pb(Xterpy)$[Au(CN)_2]^+$ linked via $Au(CN)_2^-$ units. Pb(Brterpy)$(\mu$-$OH_2)_{0.5}[Au(CN)_2]_2$ also contains a bridging water unit. In the plane of the primary crystal growth direction, the birefringence values of the four coordination polymers were found to be 0.378(19), 0.50(3), 0.38(2), and 0.26(3), respectively. The birefringence values are related to the supramolecular structures in terms of maximizing the alignment of the terpyridine-based units and the maximum off-axis positioning of the C−X bonds. With the exception of that for the Pb(Brterpy)$(\mu$-$OH_2)_{0.5}[Au(CN)_2]_2$ polymer, the birefringence values are either as large as or significantly larger than in the related M(2,2′;6′,2″-terpyridine)$[Au(CN)_2]_2$ systems. These polymers illustrate the utility of adding polarizable carbon−halogen bonds as a design element in highly birefringent coordination polymers.

Introduction

Birefringent compounds have different refractive indices (n) depending on the crystallographic direction.[1−3] These materials have a wide range of applications in nonlinear optical processes,[4−7] liquid-crystal displays,[8−10] optical filters,[11−13] and optical components such as quarter-wave plates used to form circularly polarized light.[1−3] Despite this, with the exception of liquid crystals,[14,15] the rational design and synthesis of birefringent materials has been relatively neglected, especially in inorganic chemistry, where simple inorganic compounds that have a high polarizability [e.g., calcite, the prototypical birefringent material, with a birefringence (Δn) of 0.172[3,16]] form the industry standard. Table 1 contains a list of some common inorganic solids and their birefringence values.[2,3,16]

Table 1. Birefringence Values for Some Common Inorganic Compounds

compound	Δn	compound	Δn
$CaCO_3$, calcite	0.172	H_2O, ice	0.004
$NaNO_3$	0.251	MgF_2	0.006
TiO_2, rutile	0.287	SiO_2, quartz	0.009
Hg_2Cl_2, calomel	0.683	Al_2O_3	0.027

Coordination polymers are one vehicle by which highly birefringent materials could be rationally designed and synthesized.[17,18] Coordination polymers with different properties have been developed,[20,21] including magnetic,[22,23] vapochromic,[24−28] and porous systems.[29,30] This is in part due to (a) the simple, green synthesis of these polymers in benign solvents such as

(1) Hecht, E. *Optics*, 4th ed.; Addison Wesley: San Francisco, 2002.
(2) Newnham, R. E. *Structure−Property Relations*; Springer-Verlag: New York, 1975.
(3) Newnham, R. E. *Properties of Materials: Anisotropy, Symmetry, Structure*; Oxford University Press: New York, 2005.
(4) Fiore, A.; Berger, V.; Rosencher, E.; Bravetti, P.; Nagle, J. *Nature* **1998**, *391*, 463.
(5) Zabotnov, S. V.; Konorov, S. O.; Golovan, L. A.; Fedotov, A. B.; Zheltikov, A. M.; Timoshenko, V. Y.; Kashkarov, P. K.; Zhang, H. *J. Exp. Theor. Phys.* **2004**, *99*, 28.
(6) Golovan, L. A.; Timoshenko, V. Y.; Fedotov, A. B.; Kuznestova, L. P.; Sidorov-Biryukov, D. A.; Kashkarov, P. K.; Zheltikov, A. M.; Kovalev, D.; Künzner, N.; Gross, E.; Diener, J.; Polisski, G.; Koch, F. *Appl. Phys. B: Lasers Opt.* **2001**, *73*, 31.
(7) Khoo, I. C.; Werner, D. H.; Kwon, D. H.; Diaz, A. *Mol. Cryst. Liq. Cryst.* **2008**, *488*, 88.
(8) Wu, S.-T.; Wu, C.-S. *Appl. Phys. Lett.* **1996**, *68*, 1455.
(9) Ong, H. L. *Appl. Phys. Lett.* **1991**, *59*, 155.
(10) Schadt, M. *Jpn. J. Appl. Phys.* **2009**, *48*, 03B001.
(11) Will, I.; Klemz, G. *Opt. Express* **2008**, *16*, 14922.
(12) Velasquez, P.; del Mar Sánchez-López, M.; Moreno, I.; Puerto, D.; Mateos, F. *Am. J. Phys.* **2005**, *73*, 357.
(13) Saeed, S.; Bos, P. J.; Li, Z. *Jpn. J. Appl. Phys., Part 1* **2001**, *40*, 3266.
(14) Hird, M.; Toyne, K. J.; Goodby, J. W.; Gray, G. W.; Minter, V.; Tuffin, R. P.; McDonnell, D. G. *J. Mater. Chem.* **2004**, *14*, 1731.
(15) Sekine, C.; Iwakura, K.; Minai, M.; Fujisawa, K. *Liq. Cryst.* **2001**, *28*, 1505.
(16) Weber, M. J. *Handbook of Optical Materials*; CRC Press: Boca Raton, FL, 2003.
(17) Katz, M. J.; Aguiar, P. M.; Batchelor, R. J.; Bokov, A. A.; Ye, Z.-G.; Kroeker, S.; Leznoff, D. B. *J. Am. Chem. Soc.* **2006**, *128*, 3669.
(18) Katz, M. J.; Kaluarachchi, H.; Batchelor, R. J.; Bokov, A. A.; Ye, Z.-G.; Leznoff, D. B. *Angew. Chem., Int. Ed.* **2007**, *46*, 8804.
(19) The choice of Mn(II) as a lone-pair-free substitute for Pb(II) is imperfect but not unreasonable. The ideal substitute would have been d^{10} Hg(II), an equally large, colorless cation having no lone pair, but attempts to synthesize the requisite Hg(terpy)$[Au(CN)_2]_2$ polymer were unsuccessful. Thus, d^{10} Zn(II) and d^5 Mn(II) were targeted because of the fact that these closed-shell or half-closed-shell cations are also mostly colorless; only the Mn(II) system produced high-quality crystals suitable for analysis.
(20) Janiak, C. *Dalton Trans.* **2003**, 2781.

water, methanol, and ethanol; and (b) the ease with which the materials properties of these polymers can be modified by judicious alteration of the metal cation, bridging ligand, chelating ligands, and counterions (if any).[31−33] This modularity is a critical feature that opens the door to rational design of materials with target properties.

Despite the modular nature of coordination polymer design and synthesis, there are very few reports of the measurement of the optical birefringence of coordination polymers.[17,18,34,35] These include studies of a triazolylboratesilver(I) coordination polymer ($\Delta n = 0.105$)[35] and the $Hg(CN)_2$-containing polymer $Cu(tmeda)[Hg(CN)_2]_2[HgCl_4]$ ($\Delta n = 0.0638$).[34] Our work on the synthesis of birefringent coordination polymers focused on incorporating $d^{10}s^2$ Pb(II) cations into a coordination polymer framework with $Au(CN)_2^-$, an anisotropically polarizable bridging ligand. Pb(II) was chosen for study because of (1) its high polarizability (a measure of how strongly light interacts with the atom), which is enhanced by the s^2 lone pair, coupled with (2) its lack of color in the visible spectrum (thereby facilitating birefringence measurements). Our first Pb(II)-containing coordination polymer, $Pb(H_2O)[Au(CN)_2]_2$, had a birefringence of $\Delta n = 0.070$.[17] It was immediately obvious from this result that (a) a highly birefringent coordination polymer could be synthesized with Pb(II) and $Au(CN)_2^-$ and (b) the water molecules are not highly polarizable and should be substituted with a more polarizable and anisotropic ligand. Thus, replacement of the water molecules with 2,2′;6′,2″-terpyridine (terpy) produced a coordination polymer with $\Delta n = 0.40$.[18] In order to determine the role of the coordination polymer framework, Pb(II) was replaced with Mn(II)[19] or the $Au(CN)_2^-$ was replaced with $Ag(CN)_2^-$. No significant change was observed in the birefringence of the resulting polymers, indicating that the birefringence was likely due to proper orientation of the terpy ligand by the coordination polymer framework (Figure 1).[18]

With these results in mind, our research has focused on these obvious questions: Can coordination polymers with even higher birefringence values be prepared and what methodology should be used to achieve that goal? As stated above, birefringent materials have different refractive indices in different directions.[1–3] More specifically, just as cubic, tetragonal, and orthorhombic crystals have three different, mutually perpendicular crystallographic axes (some of which may have the same magnitude, as imposed by symmetry), a birefringent compound has three mutually perpendicular refractive-index axes (two of the axes may have an equivalent refractive index, as imposed by symmetry). The principal birefringence of a sample is the difference between the refractive indices along any two of these axes (Table 1). In order to design and prepare highly birefringent coordination polymers, the factors affecting the refractive index must be understood and made as anisotropic as possible. A mathematical representation of these principles is embodied in the Lorentz−Lorenz equation (eq 1),[1]

$$n = \sqrt{\frac{1 + \frac{2\alpha N\rho}{3\,\mathrm{MW}}}{1 - \frac{2\alpha N\rho}{3\,\mathrm{MW}}}} \qquad (1)$$

in which MW is the molecular weight and N is Avogadro's number; eq 1 shows that as the polarizability (α) or density (ρ) of a material increases (along a given direction), so does the refractive index. Thus, for a birefringent material, one or both of these values must be anisotropic in the crystal lattice.

From eq 1 and Figure 1, the origin of the birefringence in $Pb(terpy)[Au(CN)_2]_2$ and $Mn(terpy)[Au(CN)_2]_2$ can be seen: the face-to-face alignment of the highly anisotropically polarizable terpy ligands by the supramolecular framework.[18] Thus, one method by which the birefringence of this prototype material can be increased is by modification of the terpy ligand to

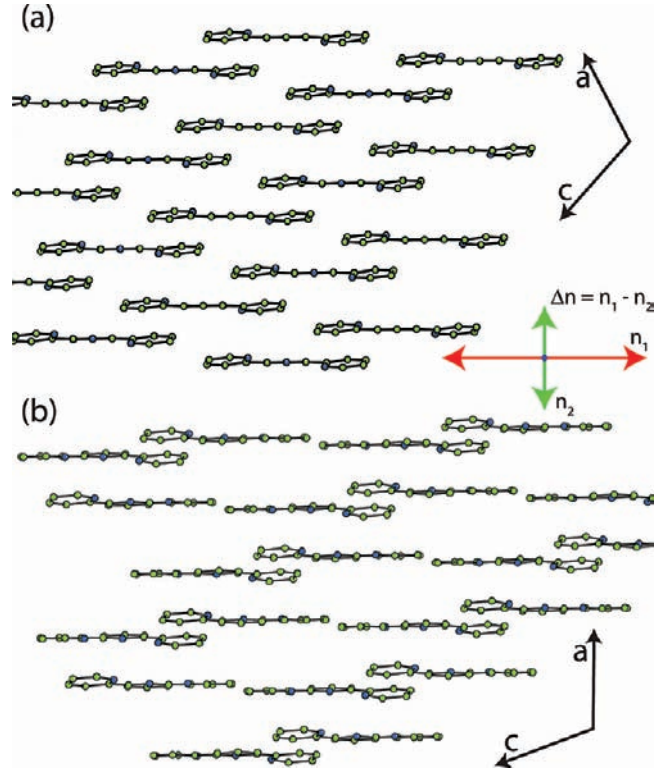

Figure 1. Terpy packing viewed down the *b* axis in the structures of (a) $Pb(terpy)[Au(CN)_2]_2$ and $Pb(terpy)[Ag(CN)_2]_2$ and (b) $Mn(terpy)[Au(CN)_2]_2$. The face-to-face alignment of the terpy ligands should be noted. The Pb(II)/Mn(II), water, and $Au(CN)_2^-/Ag(CN)_2^-$ units have been removed for clarity.

(21) Lefebvre, J.; Leznoff, D. B. In *Metal and Metalloid-Containing Polymers*; Abd-El-Aziz, A. S., Carraher, C. E., Jr., Pittman, C. U., Jr., Zeldin, M., Eds.; Wiley: New York, 2005; Vol. 5, p 155.
(22) Shatruk, M.; Dunbar, K. R. *Prog. Inorg. Chem.* **2009**, *56*, 155.
(23) Andruh, M.; Costes, J.-P.; Diaz, C.; Gao, S. *Inorg. Chem.* **2009**, *48*, 3342.
(24) Fernández, E. J.; López-de-Luzuriaga, J. M.; Monge, M.; Olmos, M. E.; Pérez, J.; Laguna, A.; Mohamed, A. A.; Fackler, J. P., Jr. *J. Am. Chem. Soc.* **2003**, *125*, 2022.
(25) Fernández, E. J.; López-de-Luzuriaga, J. M.; Monge, M.; Olmos, M. E.; Pérez, J.; Laguna, A.; Mendizabal, F.; Mohamed, A. A.; Fackler, J. P., Jr. *Inorg. Chem.* **2004**, *43*, 3573.
(26) Kato, M. *Bull. Chem. Soc. Jpn.* **2007**, *80*, 287.
(27) Lefebvre, J.; Batchelor, R. J.; Leznoff, D. B. *J. Am. Chem. Soc.* **2004**, *126*, 16117.
(28) Katz, M. J.; Ramnial, T.; Yu, H.-Z.; Leznoff, D. B. *J. Am. Chem. Soc.* **2008**, *130*, 10662.
(29) Maji, T. K.; Kitagawa, S. *Pure. Appl. Chem.* **2007**, *79*, 2155.
(30) Rosi, N. L.; Eckert, J.; Eddaoudi, M.; Vodak, D. T.; Kim, J.; O'Keeffe, M.; Yaghi, O. M. *Science* **2003**, *300*, 1127.
(31) Verdaguer, M.; Bleuzen, A.; Marvaud, V.; Vaissermann, J.; Seuleiman, M.; Desplanches, C.; Scuiller, A.; Train, C.; Garde, R.; Gelly, G.; Lomenech, C.; Rosenman, I.; Veillet, P.; Cartier, C.; Villain, F. *Coord. Chem. Rev.* **1999**, *190−192*, 1023.
(32) Chapman, K. W.; Southon, P. D.; Weeks, C. L.; Kepert, C. J. *Chem. Commun.* **2005**, 3322.
(33) Balmaseda, J.; Reguera, E.; Rodríguez-Hernández, J.; Reguera, L.; Autie, M. *Microporous Mesoporous Mater.* **2006**, *96*, 222.
(34) Draper, N. D.; Batchelor, R. J.; Sih, B. C.; Ye, Z.-G.; Leznoff, D. B. *Chem. Mater.* **2003**, *15*, 1612.
(35) Janiak, C.; Scharmann, T. G.; Albrecht, P.; Marlow, F.; Macdonald, R. *J. Am. Chem. Soc.* **1996**, *118*, 6307.

increase the anisotropy, since the primary role of the metal cations is structural. For example, the polarizability anisotropy of a $C_{ar}-Br$ bond (0.410×10^{-23} cm^3) is almost as large as that in pyridine (0.427×10^{-23} cm^3).[36] Thus, incorporating halides into the terpy ligand could potentially generate a coordination polymer that is more birefringent than the parent Pb(terpy)[Au(CN)$_2$]$_2$.[18] In order to test this design principle, substitution of the terpy ligands in M(terpy)[Au(CN)$_2$]$_2$ (M = Pb, Mn) with 4′-chloro-2,2′;6′,2″-terpyridine (Clterpy) and 4′-bromo-2,2′;6′,2″-terpyridine (Brterpy) was targeted, and the birefringence values of the resulting coordination polymers were measured. This work also presents a methodology for interpreting, in light of the structural data, the source of the high birefringence values.

Experimental Section

General Procedures. CAUTION! *Although we experienced no difficulties, perchlorate salts are potentially explosive and should only be used in small quantities and handled with care.*

Except where otherwise stated, all of the manipulations were performed in air. [^{n}Bu$_4$N][Au(CN)$_2$]·$^1/_2$H$_2$O was synthesized as previously described.[37] All of the other reagents were obtained from commercial sources and used as received.

IR spectra were recorded on a Thermo Nicolet Nexus 670 FT-IR spectrometer equipped with a Pike MIRacle attenuated total reflection (ATR) sampling accessory. Microanalyses (C, H, N) were performed by Frank Haftbaradaran at Simon Fraser University on a Carlo Erba EA 1110 CHN elemental analyzer.

Synthesis of Pb(Clterpy)[Au(CN)$_2$]$_2$. To a yellow suspension of Clterpy (27 mg, 0.10 mmol) in methanol (10 mL) was added a methanol solution (10 mL) containing Pb(ClO$_4$)$_2$·xH$_2$O (42 mg, 0.103 mmol). The solution was heated to ∼50 °C until all of the Clterpy dissolved. The resulting 20 mL solution was cooled to room temperature, after which a 20 mL methanol solution of [^{n}Bu$_4$N][Au(CN)$_2$]·$^1/_2$H$_2$O (100 mg, 0.20 mmol) was added dropwise. The solution was allowed to evaporate for several days, after which yellow crystals began to form. The solution was filtered. Although the crystals were determined to be Pb(Clterpy)[Au(CN)$_2$]$_2$, the elemental analysis indicated that the sample was not pure and likely also contained a complex with at least two Clterpy units per Pb(II). A pure sample of Pb(Clterpy)[Au(CN)$_2$]$_2$ was prepared and crystallized hydrothermally by heating Pb(NO$_3$)$_2$ (33 mg), Clterpy (27 mg), and KAu(CN)$_2$ (57 mg) to 125 °C with a 3 day cooling period. Yield: 46 mg (49%). Anal. Calcd for $C_{19}H_{10}N_5Au_2ClPb$: C, 23.45; H, 1.04; N, 10.08. Found: C, 23.42; H, 1.16; N, 10.04. IR (ATR, cm^{-1}): 3111 (w), 3095 (w), 3081 (w), 3076 (w), 3073 (w), 3061 (w), 3041 (w), 2158 (m), 2143 (s), 2139 (s), 1617 (w), 1584 (s), 1571 (m), 1550 (w), 1482 (w), 1455 (w), 1411 (s), 1337 (w), 1304 (w), 1240 (m), 1165 (w), 1130 (w), 1092 (w), 1074 (w), 1057 (w), 1048 (w), 1005 (m) 865 (m), 830 (m), 790 (s), 739 (w), 725 (m), 685 (m), 668 (w), 655 (m), 631 (w), 572 (w).

Synthesis of Pb(Brterpy)(μ-OH$_2$)$_{0.5}$[Au(CN)$_2$]$_2$. To a yellow suspension of Brterpy (31 mg, 0.10 mmol) in methanol (10 mL) was added a methanol solution (10 mL) containing Pb(ClO$_4$)$_2$·xH$_2$O (42 mg, 0.103 mmol). The solution was heated to ∼50 °C until all of the Brterpy dissolved. The resulting 20 mL solution was cooled to room temperature, after which a 20 mL methanol solution of [^{n}Bu$_4$N][Au(CN)$_2$]·$^1/_2$H$_2$O (100 mg, 0.20 mmol) was added dropwise. The solution was allowed to evaporate for several days, after which pale-yellow crystals began to form. The solution was filtered. Yield: 39 mg (38%). Anal. Calcd for $C_{19}H_{11}N_7Au_2BrO_{0.5}Pb$·0.24H$_2$O: C, 22.14; H, 1.12; N, 9.51. Found: C, 22.35; H, 1.19; N, 9.45. IR (ATR, cm^{-1}): 3097 (w), 3052 (w), 3030 (w), 3022 (w), 2927 (w), 2965 (w), 2151 (s), 2132 (s), 1592 (m), 1571 (m), 1567 (m), 1547 (m), 1479 (m), 1453 (w), 1403 (s), 1406 (s), 1298 (m), 1240 (m), 1158 (m), 1055 (w), 1009 (s), 867 (m), 789 (s), 738 (m), 727 (m), 678 (m), 655 (m), 634 (m), 558 (m), 436 (w).

Hydrothermal synthesis and crystallization of Pb(Brterpy)(μ-OH$_2$)$_{0.5}$[Au(CN)$_2$]$_2$ was also performed by heating Pb(NO$_3$)$_2$ (33 mg), Brterpy (31 mg), and KAu(CN)$_2$ (57 mg) to 125 °C followed by slow cooling to room temperature over a 3 day period. This resulted in large (at times 1 cm long) single crystals.

Synthesis of Mn(Clterpy)[Au(CN)$_2$]$_2$. To a yellow suspension of Clterpy (27 mg, 0.10 mmol) in methanol (10 mL) was added a methanol solution (10 mL) containing MnCl$_2$·4H$_2$O (20 mg, 0.10 mmol). The solution was heated to ∼50 °C until all of the Clterpy dissolved. The resulting 20 mL solution was cooled to room temperature, after which a 20 mL methanol solution of [^{n}Bu$_4$N][Au(CN)$_2$]·$^1/_2$H$_2$O (100 mg, 0.20 mmol) was added dropwise. The solution was allowed to evaporate for several days, after which yellow crystals began to form. The solution was filtered. Yield: 46 mg (57%). Anal. Calcd for $C_{19}H_{10}N_5Au_2ClMn$·0.5H$_2$O: C, 27.51; H, 1.34; N, 11.81. Found: C, 27.65; H, 1.38; N, 11.44. IR (ATR, cm^{-1}): 3488 (m, br), 3104 (w), 3085 (w), 3063 (w), 2932 (w), 2892 (w), 2819 (w), 2179 (s), 2169 (s), 2151 (s), 2144 (s), 1586 (s), 1477 (s), 1436 (w), 1415 (s), 1332 (m), 1303 (m), 1256 (s), 1243 (s), 1160 (s), 1123 (s), 1094 (m), 1045 (m), 1032 (m), 1015 (s), 910 (w), 899 (w), 877 (m), 871 (m), 825 (s), 789 (s), 751 (w), 740 (m), 727 (s), 687 (s), 656 (s).

Hydrothermal synthesis and crystallization of Mn(Clterpy)[Au(CN)$_2$]$_2$ was also performed by heating MnCl$_2$·4H$_2$O (20 mg), Clterpy (27 mg), and KAu(CN)$_2$ (57 mg) to 125 °C followed by slow cooling to room temperature over a 3 day period.

Synthesis of Mn(Brterpy)[Au(CN)$_2$]$_2$. To a yellow suspension of Brterpy (32 mg, 0.10 mmol) in methanol (10 mL) was added a methanol solution (10 mL) containing MnCl$_2$·4H$_2$O (20 mg, 0.10 mmol). The solution was heated to ∼50 °C until all of the Brterpy dissolved. The resulting 20 mL solution was cooled to room temperature, after which a 20 mL methanol solution of [^{n}Bu$_4$N][Au(CN)$_2$]·$^1/_2$H$_2$O (100 mg, 0.20 mmol) was added dropwise. The solution was allowed to evaporate for several days, after which pale-yellow crystals began to form. The solution was filtered. Yield: 44 mg (51%). Anal. Calcd for $C_{19}H_{10}N_7Au_2BrMn$: C, 26.38; H, 1.17; N, 11.33. Found: C, 26.52; H, 1.33; N, 11.13. IR (ATR, cm^{-1}): 3081 (w), 3068 (w), 2177 (s), 2147 (s), 1600 (m), 1584 (s), 1568 (s), 1552 (s), 1477 (s), 1467 (m), 1459 (w), 1410 (m), 1327 (w), 1302 (w), 1257 (w), 1244 (s), 1160 (s), 1130 (w), 1108 (w), 1096 (w), 1048 (w), 1015 (s), 862 (w), 787 (s), 741 (m), 727 (s), 682 (s), 655 (s).

Hydrothermal synthesis and crystallization of Mn(Brterpy)[Au(CN)$_2$]$_2$ was also performed by heating MnCl$_2$·4H$_2$O (20 mg), Brterpy (32 mg), and KAu(CN)$_2$ (57 mg) to 125 °C followed by slow cooling to room temperature over a 3 day period.

Single-Crystal X-ray Diffraction Structure Determinations. The crystal of Pb(Brterpy)(μ-OH$_2$)$_{0.5}$[Au(CN)$_2$]$_2$ was mounted on a MiTeGen sample holder using Paratone oil and cooled to 150 K with an Oxford cryostream for data collection. All of the other samples were mounted on glass fibers using epoxy adhesive, and the data were collected at room temperature. Additional crystallographic information can be found in Table 2.

Crystals of Pb(Clterpy)[Au(CN)$_2$]$_2$ and Mn(Clterpy)[Au(CN)$_2$]$_2$ were found to be nonmerohedral twins by an ∼180° rotation about the [100] direction in real space. The unit cells were determined using Cell_Now. Integrations were carried out using the Apex II software suite, and the subsequent absorption corrections were applied using the TWINABS software package. The space groups were determined in APEX II using the intensity data output from TWINABS. Notably, this did not affect the birefringence measurement since the 180° rotation would not change the orientation of the axes but just their direction in these specific examples. All of the other structures were processed with the Bruker APEX II

(36) Bulgarevich, S. B.; Bren, D. V.; Movshovich, D. Y.; Filippov, S. E.; Olekhnovich, E. P.; Korobka, I. V. *Russ. J. Gen. Chem.* **2002**, *72*, 1446.
(37) Lefebvre, J.; Chartrand, D.; Leznoff, D. B. *Polyhedron* **2007**, *26*, 2189.

Table 2. Crystallographic Data for Pb(Clterpy)[Au(CN)$_2$]$_2$, Pb(Brterpy)(μ-OH$_2$)$_{0.5}$[Au(CN)$_2$]$_2$, Mn(Clterpy)[Au(CN)$_2$]$_2$, and Mn(Brterpy)[Au(CN)$_2$]$_2$

	Pb(Clterpy)[Au(CN)$_2$]$_2$	Pb(Brterpy)(μ-OH$_2$)$_{0.5}$[Au(CN)$_2$]$_2$	Mn(Clterpy)[Au(CN)$_2$]$_2$	Mn(Brterpy)[Au(CN)$_2$]$_2$
empirical formula, FW	$C_{19}H_{10}N_7Au_2ClPb$, 972.92	$C_{19}H_{11.48}N_7Au_2BrO_{0.74}Pb$, 1030.71	$C_{19}H_{11}N_7Au_2ClMnO_{0.5}$, 829.66	$C_{19}H_{10}N_7Au_2BrMn$, 865.10
crystal system, space group	monoclinic, $P2_1/a$	monoclinic, $P2_1/m$	monoclinic, $P2_1/c$	monoclinic, $P2_1/c$
crystal color and habit	yellow plate	pale-yellow plate	yellow plate	pale-yellow plate
crystal size (mm^3)	0.40 × 0.34 × 0.09	0.50 × 0.41 × 0.10	0.51 × 0.16 × 0.02	0.28 × 0.13 × 0.05
a (Å)	7.873(3)	8.7680(3)	13.607(3)	9.4193(15)
b (Å)	26.978(10)	23.6668(7)	10.612(2)	25.448(4)
c (Å)	10.642(4)	11.2028(3)	32.640(7)	9.8955(16)
α (deg)	90	90	90	90
β (deg)	109.945(4)	111.505(2)	98.573(3)	113.855(2)
γ (deg)	90	90	90	90
V (Å^3)	2124.7(14)	2162.87(12)	4660.4(17)	2169.4(6)
Z	4	4	8	4
T (K)	293	150	293	293
ρ_{calcd} (g cm^{-3})	3.041	3.165	2.365	2.649
μ (mm^{-1})	21.827	23.171	13.231	15.928
R, R_w [$I_o \geq 2.50\sigma(I_o)$][a]	0.0721, 0.0819	0.0305, 0.0359	0.0496, 0.0621	0.0209, 0.0205
goodness of fit	3.5050	0.8735	1.2911	0.6134
instrument, λ (Å)	Bruker Smart Apex II, 0.71073 (Mo)			
data collection range	$2° \leq 2\theta \leq 57°$	$2° \leq 2\theta \leq 88°$	$2° \leq 2\theta \leq 57°$	$2° \leq 2\theta \leq 57°$
transmission range	0.207−0.746	0.192−0.749	0.467−0.746	0.352−0.746
final cell determination	9944 reflns (all data)	9669 reflns (all data)	3680 reflns (all data)	9932 reflns (all data)
reflections [$I_o \geq 2.50\sigma(I_o)$]	3743	6909	5837	3309
parameters, restraints	143, 0	294, 53	552, 0	272, 0

[a] Function minimized: $\sum w(|F_o| - |F_c|)^2$, where $w^{-1} = [\sigma^2(F_o) + (nF_o)^2]$ with $n = 0.010$ for Pb(Clterpy)[Au(CN)$_2$]$_2$, 0.010 for Pb(Brterpy)(μ-OH$_2$)$_{0.5}$[Au(CN)$_2$]$_2$, 0.030 for Mn(Clterpy)[Au(CN)$_2$]$_2$, and 0.010 for Mn(Brterpy)[Au(CN)$_2$]$_2$. $R = \sum||F_o| - |F_c||/\sum|F_o|$ and $R_w = [\sum w(|F_o| - |F_c|)^2/\sum w|F_o|^2]^{1/2}$.

software suite. The structures were solved with Sir92. Subsequent refinements were performed in Crystals.[38]

The C and N atoms in Pb(Clterpy)[Au(CN)$_2$]$_2$ were refined only isotropically because of limitations of the data. The structure of Pb(Brterpy)(μ-OH$_2$)$_{0.5}$[Au(CN)$_2$]$_2$ exhibited significant disorder in some of the Au(CN)$_2^-$ and water units. The bridging water molecule and the disordered cyanides on Au(2) and Au(3) were refined isotropically.

Diagrams were made using ORTEP-3,[39] POV-RAY,[40] and Cameron.[41]

Birefringence. Birefringence values were measured on plate-shaped single crystals by means of polarized-light microscopy utilizing an Olympus BX60 microscope. The optical retardation was measured using a tilting thick Berek compensator at $\lambda = 546.1$ nm at room temperature. The birefringence was calculated by dividing the measured retardation by the crystal thickness. Crystal thicknesses were measured on an FEI 235 dual-beam scanning electron microscope.

Results and Discussion

Synthesis and Structure of Pb(Clterpy)[Au(CN)$_2$]$_2$. The bulk syntheses of all of the Clterpy- and Brterpy-containing compounds were conducted in methanol. However, the resulting product of the benchtop synthesis of Pb(Clterpy)[Au(CN)$_2$]$_2$ contained a mixture of colors, and the elemental analysis indicated that the product was not pure. Switching the solvent to water was unsuccessful: mixing Pb(ClO$_4$)$_2$·xH$_2$O with Clterpy produced an immediate precipitate of Pb(Clterpy)$_x$(ClO$_4$)$_2$. On the other hand, reproducing the aqueous reaction under hydrothermal conditions produced a pure bulk product with an elemental analysis that was consistent with the crystal structure. For the other M(Xterpy)[Au(CN)$_2$]$_2$ compounds, both the ambient MeOH-based synthesis and the hydrothermal-based synthesis yielded pure products without incident. However, larger crystals were obtained hydrothermally.

The crystal structure of Pb(Clterpy)[Au(CN)$_2$]$_2$ contains a Pb(II) center with a single Clterpy ligand and four Au(CN)$_2^-$ units (Figure 2). The geometry is similar to the geometry around Pb(II) in Pb(terpy)[Au(CN)$_2$]$_2$, namely, a distorted pentagonal biprism.[18] The Pb(II)−N(pyridine) bond lengths increase from 2.572(16) to 2.610(16) Å in going from N5 to N3 (Figure 2a and Table S1 in the Supporting Information). The remaining equatorial sites around Pb(II) are surrounded by two cyanides with Pb−N(cyano) distances of 2.81(2) and 2.90(2) Å. These two Au(CN)$_2^-$ units are linked to one another via a Au2′−Au2″ interaction at a distance of 3.3232(19) Å. The axial positions on Pb(II) in Pb(Clterpy)[Au(CN)$_2$]$_2$ are occupied by two additional Au(CN)$_2^-$ units with Pb−N(cyano) bond lengths of 2.461(18) and 2.85(2) Å, which are on either side of the axial bond lengths in Pb(terpy)[Au(CN)$_2$]$_2$ [2.623(9) Å].[18] As with the majority of the Pb(II) structures reported, the bonding around Pb(II) is not symmetric because of the stereochemical lone pair on this ion.[42−50]

(38) Betteridge, P. W.; Carruthers, J. R.; Cooper, R. I.; Prout, K.; Watkin, D. J. *J. Appl. Crystallogr.* **2003**, *36*, 1487.
(39) Farrugia, L. J. *J. Appl. Crystallogr.* **1997**, *30*, 565.
(40) Fenn, T. D.; Ringe, D.; Petsko, G. A. *J. Appl. Crystallogr.* **2003**, *36*, 944.
(41) Watkin, D. J.; Prout, C. K.; Pearce, L. J. *Cameron*; Chemical Crystallography Laboratory, University of Oxford: Oxford, U.K., 1996.
(42) Shimoni-Livny, L.; Glusker, J. P.; Bock, C. W. *Inorg. Chem.* **1998**, *37*, 1853.
(43) Parr, J. *Polyhedron* **1997**, *16*, 551.
(44) Parr, J. In *Comprehensive Coordination Chemistry II: From Biology to Nanotechnology*; Parkin, G. F. R., Ed.; Elsevier Pergamon: Oxford, U.K., 2004; Vol. 3, p 545.
(45) *Lead: Chemistry, Analytical Aspects, Environmental Impact and Health Effects*; Casas, J. S., Sordo, J., Eds.; Elsevier: Amsterdam, 2006.
(46) Engelhardt, L. M.; Patrick, J. M.; Whitaker, C. R.; White, A. H. *Aust. J. Chem.* **1987**, *40*, 2107.
(47) Engelhardt, L. M.; Kepert, D. L.; Patrick, J. M.; White, A. H. *Aust. J. Chem.* **1989**, *42*, 329.
(48) Engelhardt, L. M.; Patrick, J. M.; White, A. H. *Aust. J. Chem.* **1989**, *42*, 335.
(49) Engelhardt, L. M.; Furphy, B. M.; Harrowfield, J. M.; Patrick, J. M.; Skelton, B. W.; White, A. H. *J. Chem. Soc., Dalton Trans.* **1989**, 595.
(50) Engelhardt, L. M.; Furphy, B. M.; Harrowfield, J. M.; Patrick, J. M.; White, A. H. *Inorg. Chem.* **1989**, *28*, 1410.

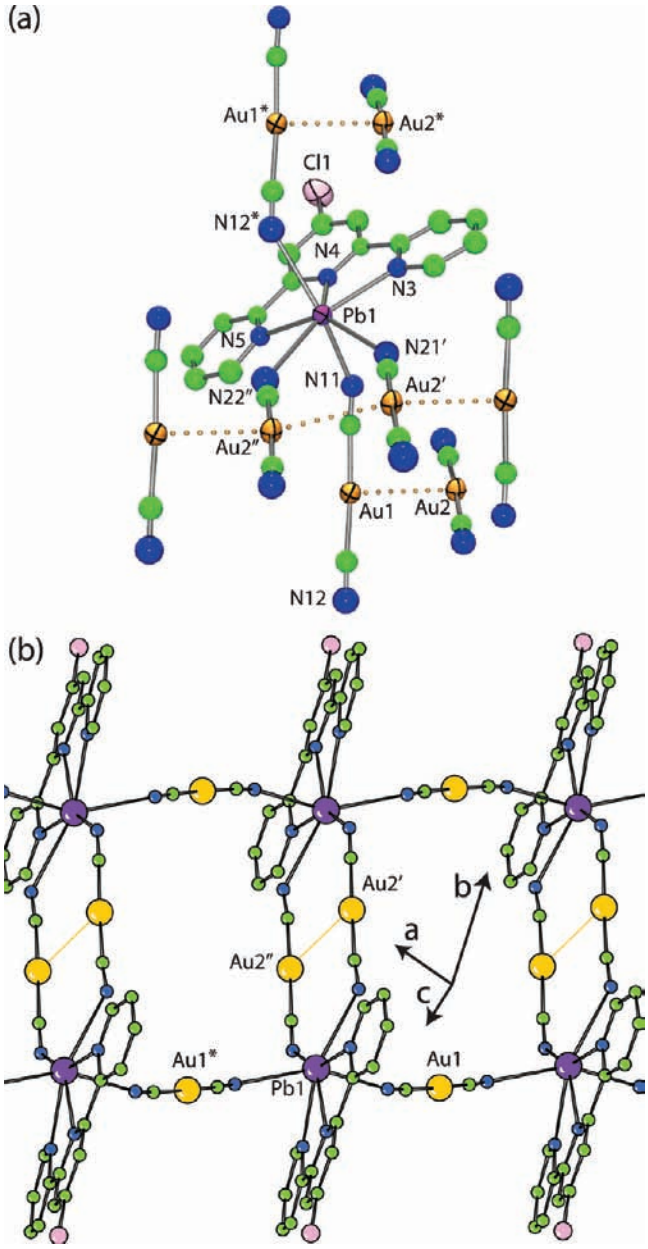

Figure 2. Crystal structure of Pb(Clterpy)$[Au(CN)_2]_2$. (a) Local geometry showing thermal ellipsoids. (b) 1D ladder structure of Pb(Clterpy)$[Au(CN)_2]_2$ showing all of the Clterpy molecules aligned face-to-face. Color scheme: Au, yellow; Pb, purple; N, blue; C, green; Cl, pink. Selected bond lengths (Å): Pb1−N21′, 2.81(2); Pb1−N12*, 2.85(2); Pb1−N22″, 2.90(2); Pb1−N3, 2.610(16); Pb1−N4, 2.592(16); Pb1−N5, 2.572(16); Pb1−N11, 2.461(18).

The extended structure of Pb(Clterpy)$[Au(CN)_2]_2$ forms a one-dimensional (1D) ladder (Figure 2b).[51] The $Pb(Clterpy)^{2+}$ units are linked to one another via the axial $Au(CN)_2^-$ units (Au1) to form 1D chains (the posts of the ladder). The equatorial cyanides (Au2) link two of the aforementioned chains to one another, forming the rungs of the ladders (Figure 2b). The ladders link to one another via 3.1011(14) Å Au−Au interactions[52−58] from the post of one ladder to the rung of a different ladder, resulting in a 2D sheet (not shown). No short

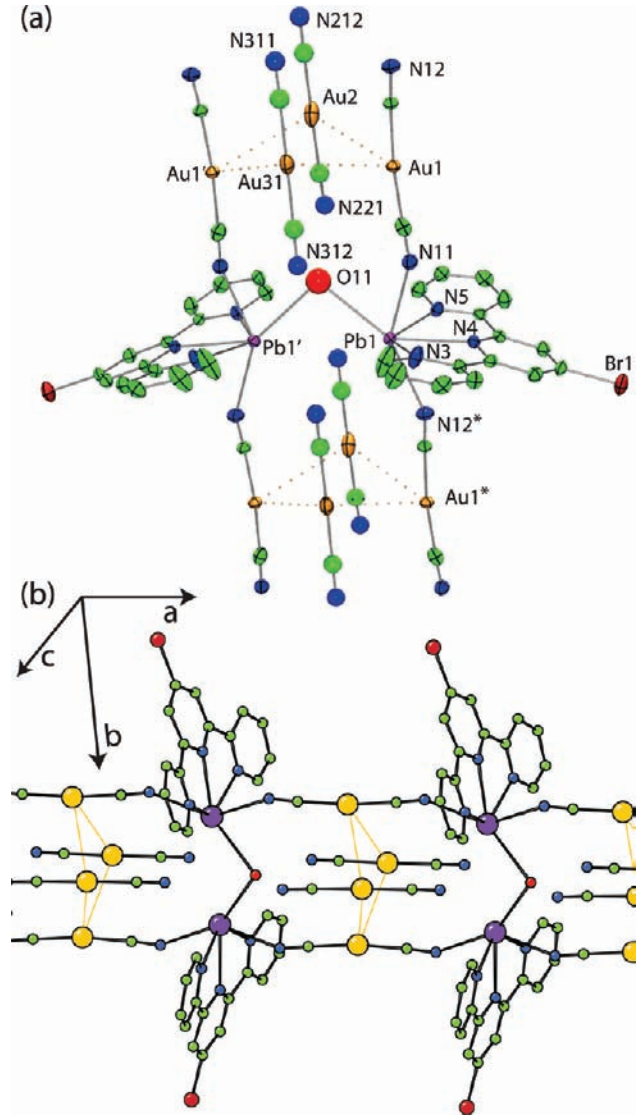

Figure 3. Crystal structure of Pb(Brterpy)$(\mu\text{-}OH_2)_{0.5}[Au(CN)_2]_2$. (a) Local geometry showing thermal ellipsoids. (b) 1D column of Pb(Brterpy)-$(\mu\text{-}OH_2)_{0.5}[Au(CN)_2]_2$. Color scheme: Au, yellow; Pb, purple; N, blue; C, green; Br, brown. Selected bond distances (Å): Pb1−N12*, 2.659(5); Pb1−O11, 2.817(6); Pb1−N3, 2.566(6); Pb1−N4, 2.589(5); Pb1−N5, 2.529(5); Pb1−N11, 2.581(5).

contacts less than the sum of the van der Waals radii are observed between neighboring 2D sheets. As with Pb(terpy)$[Au(CN)_2]_2$, all of the Clterpy units in Pb-(Clterpy)$[Au(CN)_2]_2$ are aligned face-to-face.

Structure of Pb(Brterpy)$(\mu\text{-}OH_2)_{0.5}[Au(CN)_2]_2$. The Pb(II) center in Pb(Brterpy)$(\mu\text{-}OH_2)_{0.5}[Au(CN)_2]_2$ is at least six-coordinate, as it is bound to a Brterpy unit, at least two $Au(CN)_2^-$ units, and a water molecule (Figure 3 and Table S2). The geometry is best described as a distorted octahedron. Two additional cyanide units could be considered to be bound to the Pb(II): one of the units is ∼3.3 Å away (longer than any other reported Pb−N bond lengths[59]), while the second cyanide

(51) Batten, S. R.; Robson, R. *Angew. Chem., Int. Ed.* **1998**, *37*, 1460.
(52) Bardají, M.; Laguna, A. *J. Chem. Educ.* **1999**, *76*, 201.
(53) Yam, V. W.-W.; Cheng, E. C.-C. *Top. Curr. Chem.* **2007**, *281*, 269.
(54) Balch, A. L. *Struct. Bonding (Berlin)* **2007**, *123*, 1.
(55) Stender, M.; Olmstead, M. M.; Balch, A. L.; Rios, D.; Attar, S. *Dalton Trans.* **2003**, 4282.
(56) Schmidbaur, H. *Gold Bull.* **2000**, *33*, 3.
(57) Schmidbaur, H.; Schier, A. *Chem. Soc. Rev.* **2008**, *37*, 1931.
(58) Katz, M. J.; Sakai, K.; Leznoff, D. B. *Chem. Soc. Rev.* **2008**, *37*, 1884.
(59) Harrowfield, J. M.; Miyamae, H.; Skelton, B. W.; Soudi, A. A.; White, A. H. *Aust. J. Chem.* **1996**, *49*, 1121.

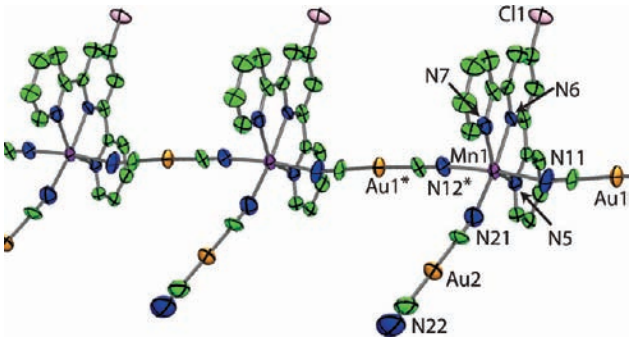

Figure 4. Crystal structure of Mn(Clterpy)[Au(CN)$_2$]$_2$ showing a 1D chain of the face-to-face-aligned terpy molecules. Color scheme: Au, yellow; Mn, purple; N, blue; C, green; Cl, pink. Selected bond distances (Å): Mn1−N12*, 2.232(11); Mn1−N5, 2.257(11); Mn1−N6, 2.216(11); Mn1−N7, 2.249(11); Mn1−N11, 2.221(11); Mn1−N21, 2.137(14).

is significantly closer but is crystallographically disordered. In one orientation, the bond length is 2.659(5) Å, and in the second orientation, the two units have a very long separation of 3.15 Å. Thus, depending on the orientation, the Pb(II) coordination may either be octahedral or distorted pentagonal bipyramidal. The Brterpy ligand is twisted from planarity, with the two outer pyridine fragments in Pb(Brterpy)(μ-OH$_2$)$_{0.5}$[Au(CN)$_2$]$_2$ bent toward each other by nearly 20°, like butterfly wings. In comparison, the same angle in Pb(Clterpy)[Au(CN)$_2$]$_2$ is less than 10°. Structures with shorter Pb(II)−terpy bond lengths have planar terpy ligands, indicating that the origin of the twist is not due to the short bond lengths.[50,60−63] The stereochemically active lone pair is more activated here than in Pb(Clterpy)-[Au(CN)$_2$]$_2$.[42–45]

The supramolecular structure of Pb(Brterpy)(μ-OH$_2$)$_{0.5}$-[Au(CN)$_2$]$_2$ contains 1D chains of Pb(Brterpy)[Au(CN)$_2$]$^+$ formed via the Au1 Au(CN)$_2^-$ unit. These chains are linked via a bridging water molecule having bond lengths of 2.817(6) Å, which is slightly shorter than the long Pb−O bond in Pb(H$_2$O)[Au(CN)$_2$]$_2$.[17] The overall structure can be considered to be a 1D column (Figure 3b).[51] Additional Au(CN)$_2^-$ units (Au2 and Au31), which, depending on the orientation, may or may not bind via μ_2-cyanides to the two Pb(II) centers, form Au−Au interactions with short and long distances of 3.3821(6) and 3.5635(4) Å, respectively, with the bridging Au(CN)$_2^-$ units of Au1.[52–58] The shortest interaction between neighboring columns is a 3.36 Å $\pi-\pi$ interaction.[64]

Structure of Mn(Clterpy)[Au(CN)$_2$]$_2$. The reaction of MnCl$_2$ with Clterpy and Au(CN)$_2^-$ in methanol produced plate-shaped crystals of Mn(Clterpy)[Au(CN)$_2$]$_2$. The structure of Mn-(Clterpy)[Au(CN)$_2$]$_2$ is similar to that of Mn(terpy)[Au(CN)$_2$]$_2$.[18] An octahedral Mn(II) is coordinated by one Clterpy ligand and three Au(CN)$_2^-$ units, two bridging and one terminal (Figure 4 and Table S3), forming a 1D half-ladder chain.[51] The difference in the structures is in the packing of these chains. In Mn-(terpy)[Au(CN)$_2$]$_2$, the chains are held together via hydrogen bonding,[18] while in Mn(Clterpy)[Au(CN)$_2$]$_2$, Au−Au interactions at a distance of 3.3018(10) Å link the rung of one half-ladder to the post of another half-ladder, forming a full 1D ladder (see Figure 6a).[51] The analogous interaction distance in Mn-(terpy)[Au(CN)$_2$]$_2$ is 3.5926(13) Å.[18]

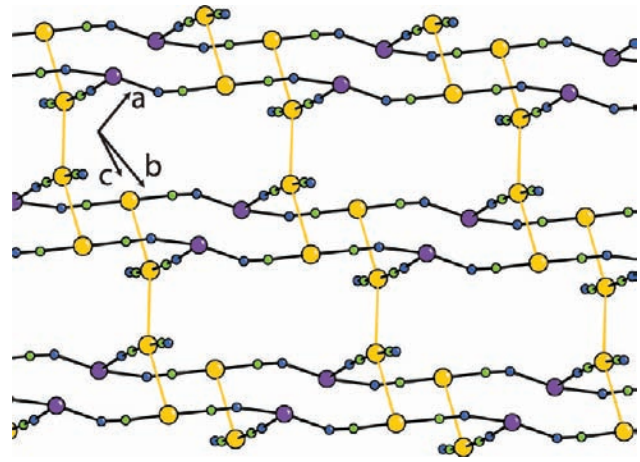

Figure 5. Crystal structure of Mn(Brterpy)[Au(CN)$_2$]$_2$ showing how 1D half-ladder chains link to form full ladder chains via Au−Au interactions. Additional Au−Au interactions link the ladders to one another. Brterpy units have been removed for clarity. Color scheme: Au, yellow; Mn, purple; N, blue; C, green. Selected bond distances (Å): Mn1−N12*, 2.230(4); Mn1−N3, 2.294(5); Mn1−N4, 2.228(4); Mn1−N5, 2.261(4); Mn1−N11, 2.241(5); Mn1−N21, 2.150(5).

As with Mn(terpy)[Au(CN)$_2$]$_2$, all of the Clterpy units in Mn(Clterpy)[Au(CN)$_2$]$_2$ are aligned face-to-face.

Structure of Mn(Brterpy)[Au(CN)$_2$]$_2$. As with Mn(terpy)-[Au(CN)$_2$]$_2$[18] and Mn(Clterpy)[Au(CN)$_2$]$_2$, the structure of Mn(Brterpy)[Au(CN)$_2$]$_2$ contains a 1D half-ladder chain of Mn(Brterpy)[Au(CN)$_2$]$_2$ units (Figure 4 and Table S4). However, unlike the chains in the terpy- and Clterpy-containing structures, which merely link to one additional half-ladder chain to form a 1D ladder, the chains of Mn(Brterpy)[Au(CN)$_2$]$_2$ link via 3.1253(5) and 3.3098(6) Å Au−Au interactions to form a 2D sheet (Figure 5).[52–58] The shorter interactions form the ladders, as in Mn(Clterpy)[Au(CN)$_2$]$_2$, while the longer interactions link neighboring ladders together (Figure 5). The array of Au atoms does not form an infinite chain but rather links four discrete Au(CN)$_2^-$ units (i.e., two ladders). The full 2D sheet is formed as different Au units along the ladder link to either the ladder above or the one below (Figure 5). The Brterpy ligands are all aligned face-to-face.

Structural Comparisons. The birefringence of a crystal is attributable to the relative orientation of the molecular components in the crystal.[2,3] For example, the birefringence of calcite is due to the face-to-face alignment of the planar carbonate anions in the crystal lattice.[1–3,65] For the view down the C_3 axis of the crystal/carbonate units, the birefringence is zero. However, for the view along the horizontal mirror plane (h) of the carbonate unit, the birefringence is 0.172. Thus, for the four Xterpy compounds presented herein, it is important to examine the 3D structural similarities and differences in order to evaluate and interpret the associated birefringence values. The first and most important global observation is that in all four compounds, the Xterpy ligands are aligned face-to-face with one another, as in Pb(terpy)[Au(CN)$_2$]$_2$.[18] As in the case of calcite,[1–3,65] this parallel ligand orientation is believed to be the primary origin of the high birefringence in Pb(terpy)[Au(CN)$_2$]$_2$.[18]

(60) Harrowfield, J. M.; Kepert, D. L.; Miyamae, H.; Skelton, B. W.; Soudi, A. A.; White, A. H. *Aust. J. Chem.* **1996**, *49*, 1147.
(61) Engelhardt, L. M.; Harrowfield, J. M.; Miyamae, H.; Patrick, J. M.; Skelton, B. W.; Soudi, A. A.; White, A. H. *Aust. J. Chem.* **1996**, *49*, 1135.
(62) Harrowfield, J. M.; Miyamae, H.; Skelton, B. W.; Soudi, A. A.; White, A. H. *Aust. J. Chem.* **2002**, *55*, 661.
(63) Harrowfield, J. M.; Miyamae, H.; Skelton, B. W.; Soudi, A. A.; White, A. H. *Aust. J. Chem.* **1996**, *49*, 1157.
(64) Janiak, C. *Dalton Trans.* **2000**, 3885.
(65) Bragg, W. L.; Langworthy, F. R. S. *Proc. R. Soc. London, Ser. A* **1924**, *105*, 370.

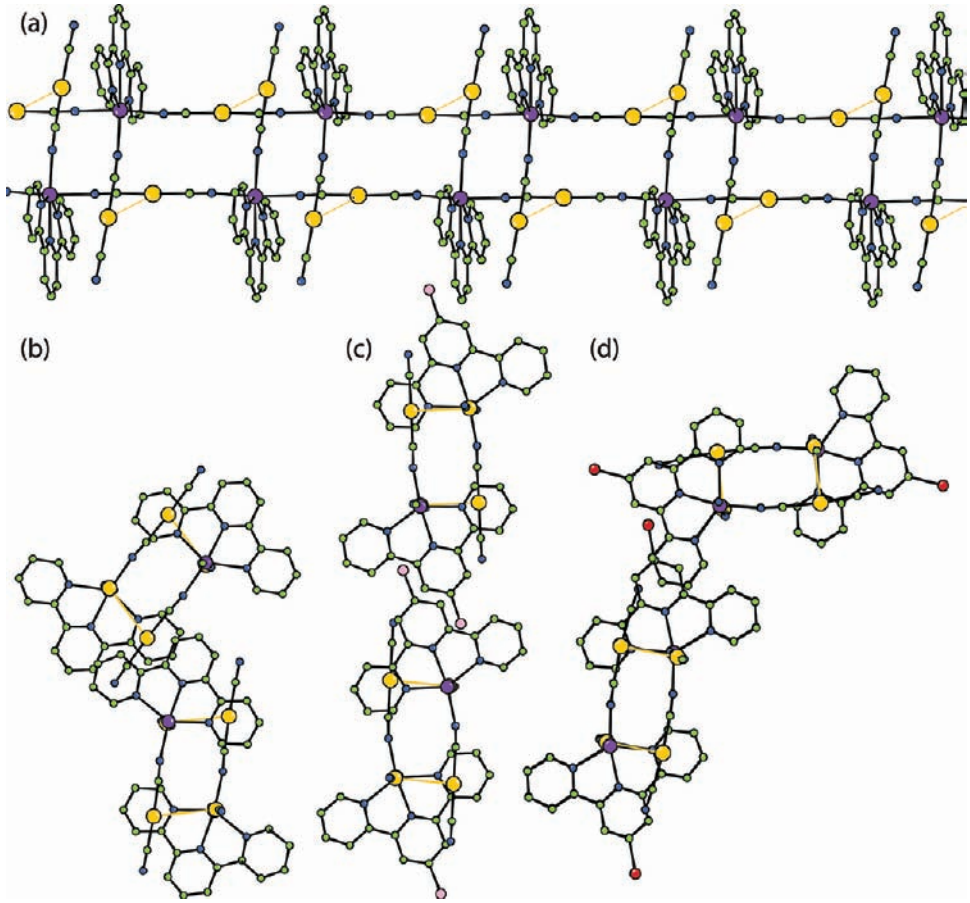

Figure 6. Structural differences between Mn(terpy)$[Au(CN)_2]_2$, Mn(Clterpy)$[Au(CN)_2]_2$, and Mn(Brterpy)$[Au(CN)_2]_2$. (a) 1D ladder of Mn(Xterpy)$[Au(CN)_2]_2$ observed in all three structures, viewed along the ladder. (b−d) Views down the 1D ladder in (a): (b) neighboring chains of Mn(terpy)$[Au(CN)_2]_2$; (c) neighboring chains of Mn(Clterpy)$[Au(CN)_2]_2$, where the presence of the Cl atom pushes neighboring ladder chains apart, leaving room for the two halves of each ladder to get closer (i.e., have shorter Au−Au interactions than in Mn(terpy)$[Au(CN)_2]_2$); (d) neighboring chains of Mn(Brterpy)$[Au(CN)_2]_2$, where the bromine pushes the neighboring atoms further apart than in Mn(Clterpy)$[Au(CN)_2]_2$, allowing for closer Au−Au interactions. Color scheme: Au, yellow; Mn, purple; N, blue; C, green; Br, brown; Cl, pink.

Substitution of terpy with Clterpy and Brterpy has surprisingly large effects on the crystal structure of the polymer. In the case of the three Mn(II)-containing structures, the basic motif is the same: a 1D half-ladder chain.[51] However, the way the rungs interact differs depending on the terpy-based ligand used. Au−Au interactions become more prevalent as the terpy ligand is substituted with Clterpy and Brterpy.[52–58] In Mn(terpy)$[Au(CN)_2]_2$, the shortest distance between neighboring gold atoms is nearly 3.6 Å, the sum of the van der Waals radii for gold.[66] In Mn(Clterpy)$[Au(CN)_2]_2$, the Au−Au interactions have a distance of 3.3 Å and link two half-ladders to form a full ladder (Figure 6a).[51] Upon substitution of Clterpy with Brterpy, the Au−Au interactions that hold the ladder together are even shorter (3.1 Å). Furthermore, unlike the terpy- and Clterpy-containing structures, the ladders in Mn(Brterpy)$[Au(CN)_2]_2$ link to one another via 3.3 Å Au−Au interactions (Figure 5).

The rationale for this observation is related to the steric constraints of the ligand on the crystal packing. As the ligands are halogen-substituted, neighboring ladders along the Mn−Cl/Br direction must be further separated to accommodate the incorporation of the halogen atom. This effect allows neighboring ladders in the perpendicular direction (Figure 6a) to come closer together, forming shorter Au−Au interactions (Figure 6b−d).

The Pb(II) structures all contain similar 1D chains of Pb(Xterpy)$[Au(CN)_2]^+$ (Figure 7a). However, it is in how these chains link to one another via an additional $Au(CN)_2^-$ unit that the structures change. Similar to Pb(terpy)$[Au(CN)_2]_2$,[18] the structures of Pb(Clterpy)$[Au(CN)_2]_2$ and Pb(Brterpy)$(\mu\text{-}OH_2)_{0.5}[Au(CN)_2]_2$ produce a 1D chain via the bridging axial $Au(CN)_2^-$ units (Au1; Figure 2). However, while the two equatorial $Au(CN)_2^-$ units in Pb(terpy)$[Au(CN)_2]_2$ form a 2D sheet[18,51] in which each chain is connected to different chains (Figure 7b), the two equatorial $Au(CN)_2^-$ units in Pb(Clterpy)$[Au(CN)_2]_2$ link to the same chain, forming a 1D ladder motif (Figures 2 and 7c). Neighboring ladders are linked to one another via short 3.1011(14) Å Au−Au interactions[52–58] that connect the rung of one ladder to the post of a different ladder (Au1 to Au2).

Comparison of the structures of Pb(Brterpy)$(\mu\text{-}OH_2)_{0.5}$-$[Au(CN)_2]_2$ and Pb(Clterpy)$[Au(CN)_2]_2$ reveals a simple relationship between the 1D chains in the two structures (Figure 7). In both structures, each Pb(Xterpy)$[Au(CN)_2]^+$ chain links to one additional chain. In Pb(Brterpy)$(\mu\text{-}OH_2)_{0.5}[Au(CN)_2]_2$, the $Au(CN)_2^-$ units that bridge these chains are rotated 90° and

(66) Bondi, A. *J. Phys. Chem.* **1964**, *68*, 441.

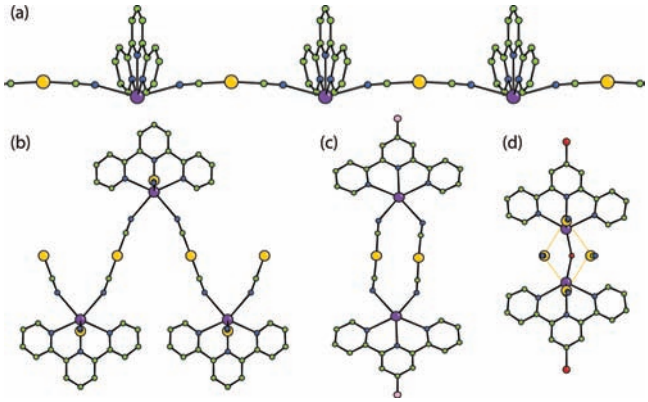

Figure 7. Structural differences between Pb(terpy)[Au(CN)$_2$]$_2$, Pb(Clterpy)[Au(CN)$_2$]$_2$, and Pb(Brterpy)(μ-OH$_2$)$_{0.5}$[Au(CN)$_2$]$_2$. (a) 1D chain of Pb(Xterpy)[Au(CN)$_2$]$^+$ observed in all three structures, viewed along the 1D chain. (b−d) Views down the 1D chain in (a): (b) each chain connects to two additional chains to make 2D sheets in Pb(terpy)[Au(CN)$_2$]$_2$; (c) each chain connects to one other chain via a bridging Au(CN)$_2^-$ unit to make a 1D ladder in Pb(Clterpy)[Au(CN)$_2$]$_2$; (d) chains connect to one other chain, this time via μ_2-cyanides of an Au(CN)$_2^-$ unit and μ_2-OH$_2$. Color scheme: Au, yellow; Pb, purple; N, blue; C, green; Br, brown; Cl, pink; O, red.

slightly shifted down the Pb(Xterpy)[Au(CN)$_2$]$^+$ chain direction relative to the bridging cyanides in Pb(Clterpy)[Au(CN)$_2$]$_2$. A water molecule also μ_2-bridges the Pb(Brterpy)[Au(CN)$_2$]$^+$ chains.

With respect to the stereochemical lone pair activity, the equatorial Pb−N(pyridine) bond lengths in Pb(terpy)[Au(CN)$_2$]$_2$ are 2.495(13) and 2.539(8) Å, and the remaining Pb−N(cyano) bond lengths are 2.623(9) (axial), and 3.016(15) Å (equatorial). With respect to Pb(terpy)[Au(CN)$_2$]$_2$, the equatorial Pb(II)−N bond lengths in Pb(Clterpy)[Au(CN)$_2$]$_2$ are longer for the Clterpy unit and shorter for the equatorial cyanide units (Figure 2 and Table S1). The shorter span in bond lengths around the Pb(II) center in Pb(Clterpy)[Au(CN)$_2$]$_2$ indicates that the stereochemical lone pair is less active than in Pb(terpy)[Au(CN)$_2$]$_2$.[42–44] Examination of the bond lengths around the Pb(II) center in Pb(Brterpy)(μ-OH$_2$)$_{0.5}$[Au(CN)$_2$]$_2$ reveals that the span of the bond lengths is significantly larger (Figure 3 and Table S2), indicating a more active stereochemical lone pair than in either the Clterpy- or terpy-based coordination polymer.

Thus, in the series of M(Xterpy)[Au(CN)$_2$]$_2$ polymers, the slightly different spatial requirements of each ligand is sufficient to alter the topology and packing, but the key feature of face-to-face-aligned Xterpy ligands that is critical for the generation of high birefringence is more-or-less preserved.[1–3,18]

Birefringence of the M(Xterpy)[Au(CN)$_2$]$_2$ Systems. All four structures crystallize in the monoclinic crystal class and are therefore biaxial;[2,3] the indicatrix (an ellipsoid representing the directional dependence of the refractive index) consists of three unique refractive index components. One of these components must lie along the *b* axis (n_b), while the other two (n_{ac1} and n_{ac2}) are perpendicular to the *b* axis and to one another, as constrained by symmetry. Unfortunately, the birefringence value that can be measured using optical microscopy is at the mercy of the primary crystal growth direction. Therefore, the measured birefringence may not represent the maximum birefringence of the sample or even the difference between two of the principal components n_b, n_{ac1}, and n_{ac2}. The birefringence of crystals that grow as thin plates perpendicular to the *b* axis represents the difference between two principal components of the indicatrix (n_{ac1} and n_{ac2}). However, if the primary growth direction is perpendicular to the *a* or *c* axis, then the measured birefringence is the difference between n_b, one of the principal components of the indicatrix (oriented along the *b* axis), and a linear combination of the remaining two principal components, n_{ac1} and n_{ac2}. In other words, the birefringence of monoclinic crystals that grow perpendicular to the *a* or *c* axis is $\Delta n = |n_b - (c_1 n_{ac1} + c_2 n_{ac2})|$, where c_j is the fractional coefficient of the corresponding refractive index. In the worst-case scenario, the crystal does not grow perpendicular to a crystallographic axis. In that case, the birefringence is merely a slice of the indicatrix with a birefringence given by $\Delta n = |(c_1 n_b + c_2 n_{ac1} + c_3 n_{ac2}) - (c_4 n_b + c_5 n_{ac1} + c_6 n_{ac2})|$.

Table 3. Crystal Growth Directions and Birefringence Values (Δn) for All of the Described Terpy-Based Coordination Polymers

polymer	growth direction	Δn
Pb(terpy)[Au(CN)$_2$]$_2$	*ac* plane	0.396(8)
Pb(terpy)[Ag(CN)$_2$]$_2$	*ac* plane	0.43(4)
Mn(terpy)[Au(CN)$_2$]$_2$	*ac* plane	0.388(8)
Pb(Clterpy)[Au(CN)$_2$]$_2$	$\perp$ to *c* axis	0.38(2)
Pb(Brterpy)(μ-OH$_2$)$_{0.5}$[Au(CN)$_2$]$_2$	*ac* plane	0.26(3)
Mn(Clterpy)[Au(CN)$_2$]$_2$	$\perp$ to *a* axis	0.378(19)
Mn(Brterpy)[Au(CN)$_2$]$_2$	$\perp$ to [11$\bar{1}$]	0.50(3)

The crystal growth directions and birefringence values of all of the compounds are summarized in Table 3.

Pb(Clterpy)[Au(CN)$_2$]$_2$. The birefringence of Pb(Clterpy)[Au(CN)$_2$]$_2$ is 0.38(2), which is not significantly different from the value obtained for Pb(terpy)[Au(CN)$_2$]$_2$.[18] Since Pb(Clterpy)[Au(CN)$_2$]$_2$ grows perpendicular to the *c* axis, one difference between the observed birefringence values of these two compounds is that the birefringence of Pb(terpy)[Au(CN)$_2$]$_2$ is the difference between two principal components of the indicatrix, while this is not necessarily true for the birefringence of Pb(Clterpy)[Au(CN)$_2$]$_2$ (as explained above).[2,3] The latter's measured birefringence represents a slice of the indicatrix containing the *b* axis [$\Delta n = |n_b - (c_1 n_{ac1} + c_2 n_{ac2})|$]. It should be noted that when a crystal is viewed between crossed polarizers it does not appear to transmit light when the principal components of the indicatrix are coplanar with the polarization planes of either of the polarizers. These positions are known as extinction positions; they appear every 90° and can be useful in determining the orientation of the indicatrix with respect to the crystal growth directions, especially when no symmetry constraints are present. To that effect, for Pb(Clterpy)[Au(CN)$_2$]$_2$, one of the extinction directions is aligned along the *b* axis (as required by symmetry). The remaining component is mutually perpendicular to the *b* axis and the *c* axis (the optical axis of the microscope). The extinction directions in Pb(Clterpy)[Au(CN)$_2$]$_2$ are thus aligned with the Clterpy twofold molecular axes (Figure 8).

Unlike the structure of Pb(terpy)[Au(CN)$_2$]$_2$, in which the twofold axes of the terpy units are perfectly aligned parallel to one another,[18] in the structure of Pb(Clterpy)[Au(CN)$_2$]$_2$, the twofold axes of the Clterpy units are not perfectly aligned down the *c* axis (Figure 8); the Clterpy units are rotated ~32° from the *c* axis. Nevertheless, the birefringence is remarkably similar to that of Pb(terpy)[Au(CN)$_2$]$_2$, despite the relatively poor alignment of the Clterpy units. The rationale for this is likely due to the projection of the C−Cl bond onto the primary crystal growth directions,[36] moreso toward the plane of the Clterpy face (pink arrows, Figure 8).

Clterpy shows the highest polarizability in the plane (face) and the lowest polarizability perpendicular to the plane (face) of the

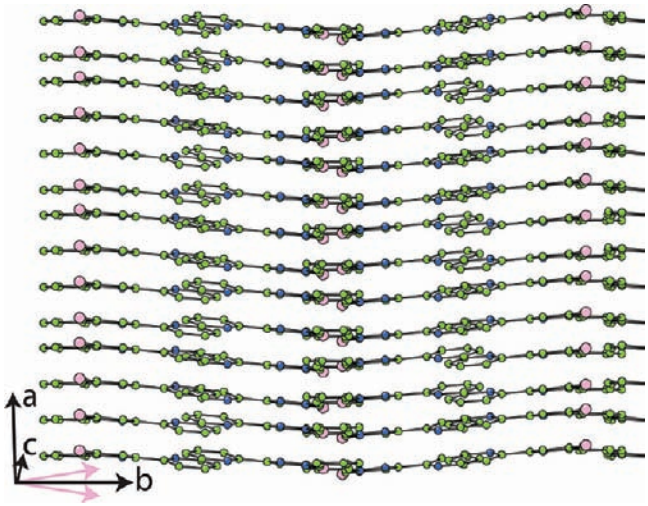

Figure 8. Crystal packing of Clterpy units in Pb(Clterpy)[$Au(CN)_2]_2$. View rotated 10° around the *b* axis, showing the face-to-face alignment of the Clterpy units. This direction is proposed to be one of the principal components of the indicatrix on the basis of the parallel alignment of the Clterpy units. The pink arrows represent the projection of the C−Cl bonds on the plane of the paper. The lengths of the arrows have been magnified for clarity; the relative size is accurate. The Pb(II) and $Au(CN)_2^-$ ions have been removed for clarity.

ligand.[36] The addition of a highly polarizable bond along the highest-polarizability direction of the ligand ultimately increases the polarizability along the *b* axis [the slow axis (i.e., the one with the larger refractive index)] of the crystal (pink arrows, Figure 8). There is less of a projection of this bond in the perpendicular direction. This is the likely rationale for why the birefringence of Pb(Clterpy)[$Au(CN)_2]_2$ is maintained as large as in Pb(terpy)-[$Au(CN)_2]_2$ despite the misalignment of the Clterpy ligands.

Pb(Brterpy)(μ-OH_2)$_{0.5}$[$Au(CN)_2]_2$. The birefringence of Pb-(Brterpy)(μ-$OH_2)_{0.5}$[$Au(CN)_2]_2$ was found to be 0.26(3), the lowest among the terpy-based polymers reported herein. The approximate extinction directions are shown as red and green arrows in Figure 9a. The slow (larger refractive index) direction is represented by the red arrow. One of the outer pyridine units is aligned with this extinction direction. Since the Brterpy ligand is not planar, the extinction direction does not align with the other two pyridine units. Furthermore, the pseudo-twofold axis of the Brterpy unit is tilted away from the *b* axis (Figure 9b). This alignment decreases the anisotropy in the *ac* plane, as it orients the ligand so the view is not down the twofold axis (the orientation of maximum birefringence for terpy). Because of the alignment of all of the Brterpy units with respect to one another (Figure 9), no other view is expected to have a significantly larger birefringence.[1–3,36,65]

Mn(Clterpy)[$Au(CN)_2]_2$. The birefringence of Mn(Clterpy)-[$Au(CN)_2]_2$ is 0.378(19), which is not significantly different from the birefringence of Mn(terpy)[$Au(CN)_2]_2$, Pb(terpy)[$Au(CN)_2]_2$, or Pb(Clterpy)[$Au(CN)_2]_2$. Crystals of Mn(Clterpy)[$Au(CN)_2]_2$ grow perpendicular to the *a* axis. Thus, one of the extinction directions is parallel to the *b* axis, while the other observed extinction direction is mutually perpendicular to the *b* and *a* axes (Figure 10). The fast (lower refractive index) axis in this case is the *b* axis. This is structurally consistent with the other terpy-based compounds. As with Pb(Clterpy)[$Au(CN)_2]_2$, the measured birefringence is not required to be the difference of two principal components of the indicatrix (by symmetry, only the *b* axis must contain a principal component of the indicatrix).

Interestingly, the birefringence of Mn(Clterpy)[$Au(CN)_2]_2$ is approximately the same as the birefringence in Mn-

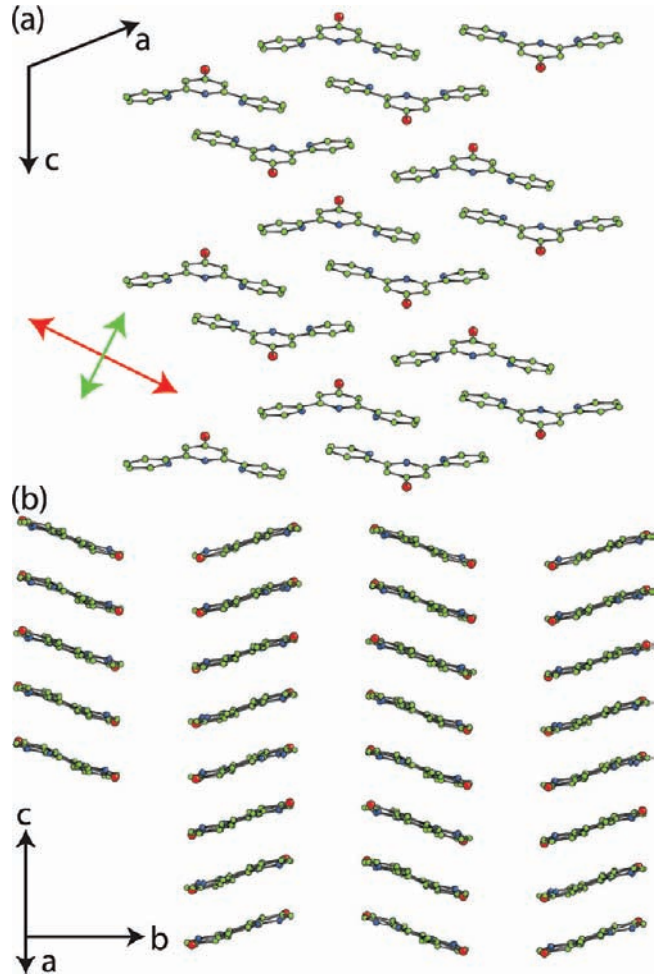

Figure 9. Crystal packing of Brterpy units in Pb(Brterpy)(μ-$OH_2)_{0.5}$[$Au(CN)_2]_2$. (a) View down the *b* axis. The red and green arrows indicate the extinction directions for this view, with the red arrow indicating the larger refractive index. (b) View perpendicular to the crystal growth direction, showing the alignment of the Brterpy units. Pb(II), $Au(CN)_2^-$, and water molecules have been removed for clarity.

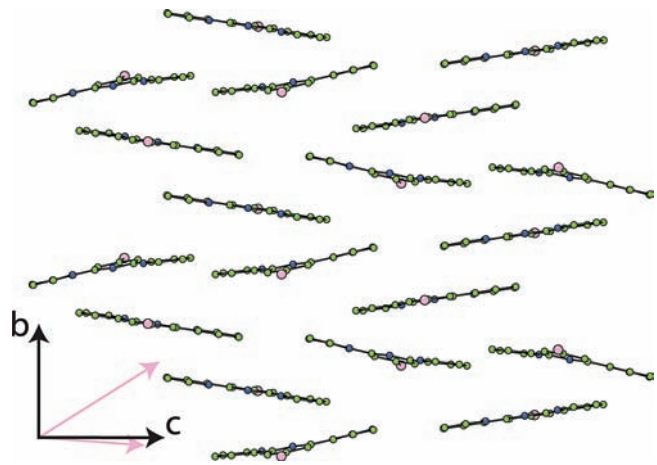

Figure 10. Crystal packing of Clterpy units in Mn(Clterpy)[$Au(CN)_2]_2$ viewed down the *a* axis, showing the alignment of the Clterpy units. The pink arrows represent the projections of the C−Cl axes on the *bc* plane. The lengths of the arrows have been magnified for clarity; the relative size is accurate. Mn(II), $Au(CN)_2^-$, and water molecules have been removed for clarity.

(terpy)[$Au(CN)_2]_2$,[18] despite the fact that the packing of the Clterpy units in Mn(Clterpy)[$Au(CN)_2]_2$ is not perfectly parallel

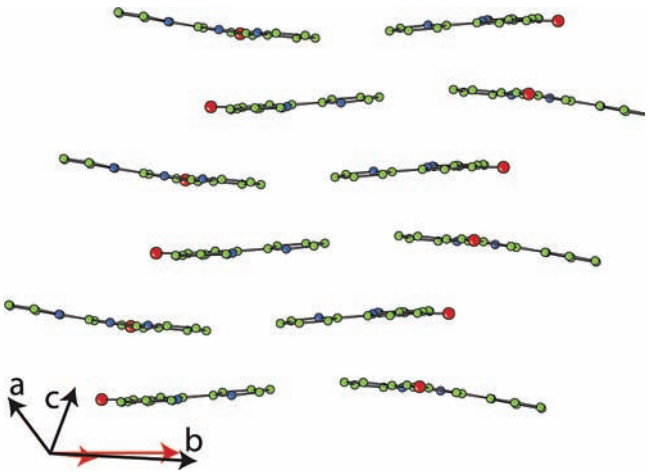

Figure 11. Crystal packing of Brterpy units in Mn(Brterpy)[Au(CN)$_2$]$_2$ viewed along the [11$\bar{1}$] axis, showing the alignment of some of the Brterpy units. The red arrows represent the projections of the C−Br axes on the (111) plane. The lengths of the arrows have been magnified for clarity; the relative size is accurate. Mn(II) and Au(CN)$_2^-$ have been removed for clarity.

(Figure 10). Neighboring chains of Mn(Clterpy)[Au(CN)$_2$]$_2$ contain Clterpy units that have a 20° twist with respect to one another (Figure 10). Furthermore, the *a* axis and the twofold axis of the Clterpy units are not parallel (8° tilt).

Because of the poorer alignment of the Clterpy units in Mn(Clterpy)[Au(CN)$_2$]$_2$ versus the alignment of the terpy units in Mn(terpy)[Au(CN)$_2$]$_2$, it would be expected that, all else being equal, the birefringence of Mn(Clterpy)[Au(CN)$_2$]$_2$ would be lower than that of Mn(terpy)[Au(CN)$_2$]$_2$. In order for the birefringence of Mn(Clterpy)[Au(CN)$_2$]$_2$ to remain as high as the birefringence of Mn(terpy)[Au(CN)$_2$]$_2$, the polarizability anisotropy in Clterpy (perpendicular to the crystal growth direction) must be larger than the polarizability anisotropy in terpy.

It is likely that this small 8° tilt is the reason the birefringence of Mn(Clterpy)[Au(CN)$_2$]$_2$ remains as high as that of Mn(terpy)[Au(CN)$_2$]$_2$. As in the structure of Pb(Clterpy)[Au(CN)$_2$]$_2$, the C−Cl bond is tilted more toward the *c* axis (the slow axis), as shown by the projection of the C−Cl bond on the *bc* plane (pink arrows, Figure 10).[36] The addition of the polarizability anisotropy of this bond in this direction likely increases the birefringence.[36] Therefore, the combination of the poor Clterpy alignment and the added polarizability anisotropy of the C−Cl bond[36] cancel one another out, so the birefringence of Mn(Clterpy)[Au(CN)$_2$]$_2$ is not significantly altered from that of Mn(terpy)[Au(CN)$_2$]$_2$.

Mn(Brterpy)[Au(CN)$_2$]$_2$. The birefringence of Mn(Brterpy)[Au(CN)$_2$]$_2$ is 0.50(3). This represents the largest birefringence value reported for a coordination polymer to date. This result supports the concept that highly birefringent materials can be rationally designed using coordination polymer synthetic methodology. Crystals of Mn(Brterpy)[Au(CN)$_2$]$_2$ grow perpendicular to the [11$\bar{1}$] direction. One of the extinction directions is along the projection of the *b* axis on the (11$\bar{1}$)-plane. The other extinction direction is mutually perpendicular to the aforementioned direction and the [11$\bar{1}$] direction. The slow axis is the projection of the *b* axis (Figure 11).

Interestingly, the crystal growth direction in Mn(Brterpy)[Au(CN)$_2$]$_2$ is not perpendicular to any of the unit cell axes. Thus, the observed birefringence is merely a slice of the indicatrix and does not indicate the maximum possible birefringence of this sample. Amazingly, despite this fact, the birefringence is larger [$\Delta n = 0.50(3)$] than those of the terpy- and other Xterpy-based coordination polymers. The Brterpy units (Figure 6) in Mn(Brterpy)[Au(CN)$_2$]$_2$ have two orientations relative to the [11$\bar{1}$] direction. The twofold axis of one Brterpy ligand is almost parallel (~10° tilt) to the [11$\bar{1}$] direction (Figure 11). The second Brterpy unit is significantly more twisted, with the twofold axis rotated ~48° away from the [11$\bar{1}$] direction (Figure 11).

Since the polarizability anisotropy of a C−Br bond is similar to that of a pyridine unit,[36] the projection of the C−Br bonds on the (11$\bar{1}$) plane (red arrows, Figure 11) is likely the source of the large birefringence, despite the "poor" alignment of the Brterpy ligands (Figure 11).

Other Factors. Although the interpretations of the sources of the high birefringence values have been argued primarily from a polarizability standpoint, there are other factors that impact the observed birefringence. For example, the density anisotropy of the sample along different directions does have some effect on the observed birefringence (eq 1). However, the impact of these variations in density can be difficult to gauge.

Conclusion

Four new coordination polymers were synthesized, and their birefringence values were measured. In line with the rational design approach for synthesizing new birefringent polymers, more polarization anisotropy was added to the terpy ligand via the addition of carbon−halogen bonds. A methodology for interpreting the measured birefringence values in terms of the 3D structures and orientations of polarizable units therein was also implemented. In Pb(Clterpy)[Au(CN)$_2$]$_2$ and Mn(Clterpy)[Au(CN)$_2$]$_2$, the addition of the halogen did not increase the birefringence. However, the substitution did maintain a high birefringence despite the relatively poorer alignment of the Clterpy units in comparison with the terpy units in Pb(terpy)[Au(CN)$_2$]$_2$. When the more polarizable Brterpy ligand was used, the birefringence of Pb(Brterpy)(μ-OH$_2$)$_{0.5}$[Au(CN)$_2$]$_2$ decreased significantly because of the structure and subsequent relatively poor alignment of the Brterpy units. However, in the Mn(Brterpy)[Au(CN)$_2$]$_2$ polymer, the birefringence was larger than that of its terpy predecessor, Mn(terpy)[Au(CN)$_2$]$_2$, and represents one of the highest birefringence values for solids reported to date. The increase in birefringence was attributed to the presence of a C−Br bond that is well-aligned in the measurement plane. Thus, the presence of highly polarizable halogen atoms can be used to increase the birefringence of a coordination polymer if the halogen substitution position is judiciously chosen and properly aligned by the polymer framework/packing. This provides valuable guidance for the rational design of more highly birefringent coordination polymer materials, a new class of compounds that now contains some of the most highly birefringent solids reported to date.

Acknowledgment. The authors thank the NSERC of Canada, the Natural Resources Canada Internship program (M.J.K.), and the World Gold Council GROW program for financial support.

Supporting Information Available: Single-crystal X-ray crystallographic data (CIF) and tables of bond lengths and angles for all four coordination polymers. This material is available free of charge via the Internet at http://pubs.acs.org.

JA907519C